Fall back accretion and energy injections in the ultra-long GRB 111209A

Y. B. Yu[1,2], X. F. Wu[3,4,5], Y. F. Huang[1,6], D.M. Coward[2,7], G. Stratta[8], B. Gendre[8,9], and E.J. Howell[2]

ABSTRACT

The ultra-long Gamma Ray Burst 111209A, which occurred at a redshift of $z = 0.677$, is the longest duration burst ever observed due to a rest frame prompt emission duration of order of 10^4 s. The very early X-ray afterglow of Gamma Ray Burst 111209A showed unusual behavior, with a significant bump observed at about 2000 s after the BAT trigger. One possible explanation is that the bump resulted from mass fall back. In this paper, we present a detailed numerical study of the fall back process to interpret the very early X-ray afterglow light curve of Gamma Ray Burst 111209A. For the afterglow at late times, we apply external shock by adding an energy injection. In our model, we assume two periods of energy injection, each with a constant injection power. One injection starts at 8.0×10^3 s and lasts for about 8000 s, with an injection power of 9.0×10^{47} erg s^{-1}; this energy injection accounts for the plateau at X-ray wavelength in the early stage. The other injection starts at 6.5×10^4 s and lasts for about 16 ks with an injection power of 6.0×10^{46} erg s^{-1}. This second energy injection can help to explain the other plateau at X-ray wavelengths and the rebrightening in the optical band at about 10^5 s. We argue that the two periods of energy injection can be produced by the infall of clumpy mass onto the central compact object of the burster, which leads to an enhancement of the accretion rate and results in a strong temporary outflow.

Subject headings: gamma rays: bursts – ISM: jets and outflows – stars: individual (GRB 111209A)

[1]Department of Astronomy, Nanjing University, Nanjing 210093, China; hyf@nju.edu.cn

[2]School of Physics, University of Western Australia, Crawley WA 6009, Australia; David.Coward@uwa.edu.au

[3]Purple Mountain Observatory, Chinese Academy of Sciences, Nanjing 210008, China; xfwu@pmo.ac.cn

[4]Chinese Center for Antarctic Astronomy, Chinese Academy of Sciences, Nanjing 210008, China

[5]Joint Center for Particle Nuclear Physics and Cosmology of Purple Mountain Observatory-Nanjing University, Chinese Academy of Sciences, Nanjing 210008, China

[6]Key Laboratory of Modern Astronomy and Astrophysics (Nanjing University), Ministry of Education, China

[7]Australian Research Council Future Fellow

[8]Osservatorio Astronomico di Roma (OAR/INAF), via Frascati 33, 00040, Monte Porzio Catone, Italy

[9]ARTEMIS, Observatoire de la Côte d'Azur, FRANCE

1. Introduction

Gamma-ray bursts (GRBs) are bright flashes of high-energy photons coming from random directions in the sky at random times (for recent reviews, see Zhang 2007; Gehrels et al. 2009), typically lasting for tens of seconds (Klebesadel et al. 1973). The external shock model is very successful and popular in view of the fact that it can explain the main features of GRB afterglows well (Rees & Mészáros 1994; Piran 1999; Zhang 2007), which are generally believed to arise from the interaction of the GRB relativistic outflow with the surrounding environment medium (Mészáros & Rees 1997a; Piran 2000; Mészáros 2002). Based on duration and spectrum, there are two main classes of GRBs with well separated properties and behaviors, long GRBs and short GRBs. After the amazing coincidence of GRB 980425 and SN 1998bw (Galama et al. 1998), significant observational evidence has supported the hypothesis that long GRBs are associated with Type Ic supernovae which result from the collapse of Wolf-Rayet (WR) stars (for a recent review, see Bersier 2012). Since the accretion timescale of the WR star envelope onto the central engine is consistent with the typical observed durations of long GRBs, which are tens of seconds, it is believed that long GRBs should be due to the collapse of massive stars (Woosley 1993; Paczyński 1998; MacFadyen & Woosley 1999) and WR stars are the most plausible progenitors (Chevalier & Li 1999). At the same time, it is also widely accepted that short GRBs could be connected with the coalescence of two compact objects (Eichler et al. 1989; Narayan et al. 1992; Gehrels et al. 2005; Nakar 2007), such as neutron star (NS) - black hole (BH) or NS-NS mergers (Janka et al. 1998; Bloom et al. 1999; Perna & Belczynski 2002; Bethe et al. 2007; Tutukov & Fedorova 2007). Before the remnant of NS-NS mergers collapse to a BH, it is predicted that they will form an unstable millisecond pulsar (magnetar), which powers a plateau phase in the X-ray light curve. Recently, more and more observations and simulations support this prediction (Fan & Xu 2006; Dall'Osso et al. 2011; Rowlinson et al. 2013), indicating that magnetar may be the central engine of short GRBs (Kluźniak & Ruderman 1997).

With the development of new observational techniques, especially after the launch of the Swift satellite, many unexpected features have been observed in GRB afterglows, such as strong or multiple flares at X-ray wavelength, and quick or high amplitude rebrightenings in optical band (for a recent review, see Zhang 2007). GRB 111209A is one of the most interesting events, because it has a significant bump at X-ray wavelength and a remarkable rebrightening in its optical afterglow light curve. Another example of a burst with significant X-ray rebrightening is GRB 121027A, with a redshift of $z = 1.773$ measured by identifying several metal absorption lines with the X-shooter spectragraph (Kruehler et al. 2012). Since X-ray flares share a lot of similarities with GRB prompt emission, they are usually interpreted as due to internal shocks (Burrows et al. 2005; Zhang et al. 2006; Fan & Wei 2005), which is the well known mechanism for prompt emission. However, GRB 121027A is so special that its X-ray afterglow rebrightened sharply at about 1000 s after the trigger by more than two orders of magnitude in less than 200 s and lasted for more than 10^4 s, which is quite different from typical X-ray flares, indicating a different physical origin. Wu et al. (2013) proposed a fall back accretion model within the context of the collapse of a massive star for a long

duration GRB to explain the sharp rise of the X-ray flare with falling back mass $M_{\rm fb} \sim 0.9-2.6 M_{\odot}$ from the radius $r_{\rm fb} \sim 3.5 \times 10^{10}$ cm. As discussed by Stratta et al. (2013), for GRB 111209A, internal shock has problems to explain the spectral lag between the optical and high energy start time of the flare observed in the early stage. In this paper, we apply the fall back accretion model to GRB 111209A and interpret the significant bump observed in X-ray band at about 2000 s after the BAT trigger.

For exceptional rebrightenings in optical band, other examples include GRB 060206 (Wózniak et al. 2006) and GRB 970508 (Sokolov et al. 1999). These rebrightenings are obviously inconsistent with the simple form of power-law decay as predicted by the standard external shock model with synchrotron emission coming from the forward shock of ejecta ploughing into an external medium (Rhoads 1999; Sari et al. 1999). Many different mechanisms have been proposed to explain the rebrightenings, including the density jump model (Dai & Lu 2002; Lazzati et al. 2002; Dai & Wu 2003; Tam et al. 2005), the energy injection model (Dai & Lu 1998; Rees & Mészáros 1998; Huang et al. 2006; Dall'Osso et al. 2011; Yu & Huang 2013; Geng et al. 2013), the two-component jet model (Huang et al. 2004; Liu et al. 2008), and the microphysics variation mechanism (Kong et al. 2010), etc. However, in the more detailed numerical simulations, Huang et al. (2007) argued that the density jump model is usually not an ideal mechanism to produce the rebrightenings in optical afterglows.

Interestingly, Nakauchi et al. (2013) reproduced some of the X-ray and optical/infrared afterglow light curves reasonably well with the standard external shock model. In their model, the prompt gamma-ray emissions and the standard afterglow emissions are attributed to a relativistic jet, while the superluminous-supernova like bump comes from a non-relativistic cocoon fireball. But their calculations still failed to reproduce the plateau at X-ray wavelength and the rebrightening in the optical band at about 10^5 s. Energy injection from late and slow shells seems to be a natural interpretation for the rebrightening of many optical afterglows. Especially, GRB 970508 exhibited a late-time flare similar to what is expected from colliding shells (Sokolov et al. 1999).

In this study, we will use the energy injection mechanism to explain the unusual X-ray and optical afterglow light curves of GRB 111209A at late times. In our calculation, we only consider the synchrotron emission, which is the dominant radiation mechanism that takes place in the afterglow stage, although inverse Compton scattering may also play a role in some cases (Wei & Lu 2000; Sari & Esin 2001).

The outline of our paper is as follows. The observations are summarized in Section 2. The mass fall back accretion model and the external shock with energy injection process, including the dynamics and the radiation process, are described in Section 3. In Section 4, we calculate the overall dynamical evolution of the outflow numerically, and reproduce the unusual X-ray and optical afterglow light curves of GRB 111209A. It is shown that the observed bump and plateaus at X-ray wavelength and rebrightening in the optical band can be well reproduced. Finally, in Section 5, we summarize our results and give a brief discussion. We use the following cosmological

parameters, $H_0 = 71$ km s^{-1} Mpc^{-1}, $\Omega_M = 0.27$ and $\Omega_\Lambda = 0.73$, throughout the paper.

2. Data

In this section, we summarize the multi-wavelength observational results of GRB 111209A. At 07:12:08 UT on Dec 09 2011, GRB 111209A triggered the Burst Alert Telescope (BAT) onboard the Swift satellite and was located at coordinates $RA(J2000) = 00^h57^m22.63^s, Dec(J2000) = -46°48'03.8''$, with an estimated uncertainty of 0.5 arcsec (Hoversten et al. 2011). The 1-sec peak photon flux of GRB 111209A measured by the BAT in the 15 – 150 keV band was 0.5 ± 0.1 ph cm^{-2} s^{-1} with the intrinsic peak of the spectrum $E_{\rm p} = 520 \pm 89$ keV. The X-ray spectrum at about 5 days was best fit by a simple power law with a spectral index of $\beta_X = 1.8 \pm 0.4$ (Stratta et al. 2013), which is consistent with the expectation of the external shock model for fast cooling electrons (Sari et al. 1998). The redshift measured by the X-shooter spectrograph mounted at the Kueyen unit of the VLT on Cerro Paranal from several absorption features in the host galaxy of GRB 111209A was z = 0.677 (Vreeswijk et al. 2011). The luminosity distance of GRB 111209A is then 4.1 Gpc. A number of ground-based telescopes performed follow-up observations, providing the multi-frequency light curves of the afterglow. GRB 111209A was an unusual event with unusual X-ray and optical afterglow light curves among the GRBs. One of the most remarkable features of this burst is that the X-ray afterglow light curve has a significant bump at around 2000 s.

2.1. Early X-ray emission

The XRT onboard the Swift satellite started to observe GRB 111209A 425 s after the BAT trigger (Hoversten et al. 2013), revealing a bright afterglow, which was also detected by UVOT in the optical-UV bands. The X-ray afterglow light curve shows a shallow initial decay phase lasting for about 2000 s and the best fit decay index is $\alpha = 0.544 \pm 0.003$ (Gendre et al. 2013). What makes the X-ray afterglow light curve of GRB 111209A unusual is the significant bump beginning at about 2000 s after the BAT trigger. At the end of the shallow decay phase, the X-ray afterglow light curve evolved into the so called steep decay phase, which corresponds to the true end of the prompt phase and is usually interpreted as the high latitude emission of the prompt phase (Kumar & Panaitescu 2000). The steep decay of the X-ray light curve could be described by a simple power law ($f_\nu = t^{-\alpha}$) and the best-fit model has a decay index of $\alpha = 4.9 \pm 0.2$ (Gendre et al. 2013). The Swift/XRT spectrum could be described by a broken power law function and the best-fit model has a photon index of 1.2 and 2.1, with a break energy of 3.1 keV. According to Gendre et al. (2013), the prompt spectrum of GRB 111209A shows a thermal component at the start of the XRT observation, but it disappeared very soon, and most of the prompt phase is free of thermal emission.

2.2. Afterglows at late times

Gendre et al. (2013) activated a Target of Opportunity observation with XMM-Newton between 56664 s and 108160 s, which covered the end of the prompt phase and the start of the normal afterglow decay phase. Because of the better sensitivity of XMM-Newton in comparison with the Swift/XRT, the exceptionally high quality of XMM data revealed the presence of a plateau at the end of the steep decay. The X-ray afterglow light curve after the steep decay phase can be modeled with a broken power law, a plateau with the decay index of 0.5 ± 0.2 and a normal decay with the index of 1.51 ± 0.08 (Gendre et al. 2013). The Swift/UVOT began observing the afterglow of GRB 111209A at 427 s after the BAT trigger, and the afterglow was detected in all seven UVOT filters, indicating that the redshift should be $z < 1.6$, which is consistent with the final reported redshift of $z = 0.677$ (Vreeswijk et al. 2011). The R band light curve shows many interesting features, and is very different from the optical afterglow of a typical GRB. The initial light curve decayed in the normal way with the simple power-law extrapolation, but the afterglow rebrightened significantly and rapidly at about 10^5 s after the trigger, interrupting the smooth early-time temporal evolution, which cannot be explained by using the standard external shock model. The observed light curve confirmed the rebrightening from $r' \sim 20.9$ magnitude to a peak value of $r' \sim 20.0$ magnitude, probably implying the release of a large amount of energy at late times.

3. Model

3.1. Mass fall back accretion model

Wu et al. (2013) proposed a mass fall back accretion model to interpret the step-like rebrightening of the X-ray afterglow of GRB 121027A observed at about 1000 s since the burst with a duration of more than 10^4 s. As suggested by Wu et al. (2013), in the fall back accretion model, the central engine will be provided by a BH. Blandford-Znajek (BZ) mechanism powers GRB jet by extracting the rotational energy of Kerr BH through large-scale magnetic field. During the last stage of evolution of the progenitor, a significant proportion of the helium envelope that have survived mass loss will undergo fall-back and accretion of the stellar envelope may produce the X-ray bump seen in some GRBs. In this paper, we will use the mass fall back process to interpret the very early X-ray afterglow light curve of GRB 111209A. For completeness, we first describe the fall back accretion model briefly (for details, see Wu et al. 2013). According to Wu et al. (2013), the evolution of mass ($M_\bullet$), angular momentum ($J_\bullet$) and spin ($a_\bullet$) of the BH are described as

$$\frac{dM_\bullet c^2}{dt} = \dot{M} c^2 E_{\rm ms} - \dot{E}_B, \tag{1}$$

$$\frac{dJ_\bullet}{dt} = \dot{M} L_{\rm ms} - T_B, \tag{2}$$

$$\frac{da_\bullet}{dt} = (\dot{M} L_{\rm ms} - T_B) c/(G M_\bullet^2) - 2a_\bullet (\dot{M} c^2 E_{\rm ms} - \dot{E}_B)/(M_\bullet c^2), \tag{3}$$

where $\dot{M}$, $\dot{E}_B$ and T_B are the fall back accretion rate, BZ jet power and total magnetic torque applied on the BH, respectively. $E_{\rm ms}$ and $L_{\rm ms}$ are the specific energy and angular momentum, respectively, given as (Novikov & Thorne 1973)

$$E_{\rm ms} = \frac{4\sqrt{R_{\rm ms}} - 3a_\bullet}{\sqrt{3}R_{\rm ms}}, \tag{4}$$

$$L_{\rm ms} = \frac{GM_\bullet}{c}\frac{2(3\sqrt{R_{\rm ms}} - 2a_\bullet)}{\sqrt{3R_{\rm ms}}}, \tag{5}$$

where $R_{\rm ms}$ is the radius of the marginally stable orbit, given through the expression (Bardeen et al. 1972)

$$R_{\rm ms} = 3 + Z_2 - [(3 - Z_1)(3 + Z_1 + 2Z_2)]^{1/2}, \tag{6}$$

with $Z_1 \equiv 1 + (1 - a_\bullet^2)^{1/3}[(1 + a_\bullet)^{1/3} + (1 - a_\bullet)^{1/3}]$, $Z_2 \equiv (3a_\bullet^2 + Z_1^2)^{1/2}$ for $0 \leq a_\bullet \leq 1$.

The mass fall back accretion rate initially increases with time as $\dot{M} \propto t^{1/2}$ (MacFadyen et al. 2001; Zhang et al. 2008; Dai & Liu 2012), and the late-time fall back accretion behavior follows $\dot{M} \propto t^{-5/3}$ (Chevalier 1989) with a break time $t_{\rm p}$; therefore, we take the same smooth-broken-power-law function of the fall back accretion rate as assumed by Wu et al. (2013)

$$\dot{M} = \dot{M}_{\rm p}[\frac{1}{2}(\frac{t - t_0}{t_{\rm p} - t_0})^{-\alpha_r s} + \frac{1}{2}(\frac{t - t_0}{t_{\rm p} - t_0})^{-\alpha_d s}]^{-1/s}, \tag{7}$$

where $\alpha_{\rm r} = 1/2$, $\alpha_{\rm d} = -5/3$ and s describes the sharpness of the peak. $\dot{M}_{\rm p}$ is the accretion rate at $t_{\rm p}$ and t_0 is the start time of fall back. The BZ jet power from a BH with mass $M_\bullet$ and angular momentum $J_\bullet$ is (Lee et al. 2000; Wang et al. 2002; Mckinney 2005; Lei & Zhang 2011)

$$\dot{E}_B = 1.7 \times 10^{50} a_\bullet^2 M_\bullet / {M_\odot}^2 B_{\bullet,15}^2 F(a_\bullet) \text{ erg s}^{-1}, \tag{8}$$

where $B_{\bullet,15} = B_\bullet/10^{15}$ G and

$$F(a_\bullet) = ((1 + q^2)/q^2)((q + 1/q)\arctan q - 1). \tag{9}$$

Here $q = a_\bullet/(1 + \sqrt{1 - a_\bullet^2})$.

3.2. External shock

In recent years, van Eerten et al. (2010) developed a code for the dynamical evolution of GRB afterglows. Their calculations included some delicate ingredient and are relatively accurate. However, their code is also relatively complicated. Here we use the simple equations for beamed GRB ejecta developed by Huang et al (1998, 1999a, 1999b, 2000a, 2000b) to describe the dynamic and radiation process of the afterglows of GRB 111209A at late times. These equations are applicable to both radiative and adiabatic blastwaves, and are appropriate for both ultra-relativistic and non-relativistic stages (Huang & Cheng 2003). Additionally, it takes the lateral expansion,

the cooling of electrons, and the equal arrival time surface effect into consideration. However, note that if some subtle effects such as the adiabatic pressure and radiative losses were considered, then the dynamics could be slightly different (Pe'er 2012; Nava et al. 2013).

In the standard external shock frame work, as the blast wave sweeps up the surrounding medium, the shock accelerates electrons. The afterglow emission arises from synchrotron radiation of these shocked electrons due to their interaction with magnetic fields. Considering the energy injection, the differential equations should be modified accordingly so that they can be applied to GRB 111209A. Due to strong magnetic field and rapid rotation, a new-born millisecond pulsar will lose its rotation energy through magnetic dipole radiation. Dai & Lu (1998) have considered the energy injection from a new-born strongly magnetized millisecond pulsar at the center of GRB. They argued that the radiation power evolves with time as $L(t) = L_0(1 + t/T)^{-2}$, where L_0 is the initial luminosity, t is the time in the burster's rest frame, and T is the spin-down timescale. Considering an adiabatic relativistic hot shell which receives the energy injection from the central engine through a Poynting-flux-dominated flow, Zhang & Mészáros (2001b) assumed an intrinsic luminosity law, *e.g.* $L(t) \propto t^q$, where t is the intrinsic time of the central engine. They pointed out that usually $q = 0$ during the injection phase in many cases. To explain the special behaviors of GRB 070610 in the observed X-ray and optical afterglow light curves, Kong & Huang (2010) assumed that the energy injection power takes the form of $dE_{\rm inj}/dt = Qt^q$ for $t_{\rm start} < t < t_{\rm end}$, where Q and q are constants, $t_{\rm start}$ is the beginning time of the energy injection, and $t_{\rm end}$ is the ending time of the energy injection. For some types of central engines, such as a black hole plus a long-lived debris torus system, the energy injection to the external shock may in principle continue for a time scale significantly longer than that of the gamma-ray emission (Zhang & Mészáros 2001a).

In our case, the central engine of the ultra-long GRB 111209A is a BH, suggesting the energy injection should be from the fall back process. Taking into account all the energy injection forms as described above, and the extremely fast optical rebrightening of the afterglow of GRB 111209A at about 10^5 s after the trigger time, here we take the same form of energy injection power as Kong & Huang (2010). The differential equation for the evolution of the bulk Lorentz factor should then be changed to

$$\frac{d\gamma}{dt} = \frac{1}{M_{ej} + \epsilon m + 2(1-\epsilon)\gamma m} \times (\frac{1}{c^2}\frac{dE_{inj}}{dt} - (\gamma^2 - 1)\frac{dm}{dt}). \quad (10)$$

where M_{ej} is the initial ejecta mass, m is the swept-up interstellar medium (ISM) mass, and ϵ is the radiative efficiency. In the following, we take the simplest case, $q = 0$.

4. Numerical Results

4.1. Early X-ray emission

For GRB 111209A, the X-ray bump appears at about 2000 s, which corresponds to a rest frame duration $t_0 \sim 1200\ s$; this suggests the minimum radius around which matter starts to fall back is

$$r_{\rm fb} \simeq 7.7 \times 10^{10} (M_\bullet/3M_\odot)^{1/3} (t_0/1200\ s)^{2/3}\ {\rm cm}, \tag{11}$$

The total rising time of the bump is about 1100 s, which corresponds to $t_{\rm p} - t_0 \sim 1100/(1+z)\ s \sim 650$ s, suggesting the total accreted mass should be

$$M_{\rm fb} \simeq 2\dot{M}_{\rm p}(t_{\rm p} - t_0)/3 \simeq 1.6 \times 10^{-2} L_{\rm X,iso,50} a_\bullet^{-2} X^{-1}(a_\bullet) \eta_{-2}^{-1} f_{\rm b,-2} M_\odot, \tag{12}$$

where $L_{\rm X,iso,50} = L_{\rm X,iso}/10^{50}$ and $X(a_\bullet) = F(a_\bullet)/(1+\sqrt{1-a_\bullet^2})^2$. $\eta_{-2} = \eta/10^{-2}$ and $f_{\rm b,-2} = f_{\rm b}/10^{-2}$ are the efficiency of converting BZ power to X-ray radiation and the beaming factor of the jet respectively.

We obtain the time evolution of the BZ power by carrying out numerical calculation of Eqs.(1) - (9), and compare it with the observations of the X-ray bump in GRB 111209A. The parameter of the beaming factor was taken as $f_{\rm b} = 0.01$, corresponding to a half opening angle of $\theta = 0.1$ radian, which is the lower limit given by the non-detection of the jet break in the X-ray afterglow. A complete monitoring before and after the flare peak epoch at about 2000 s since the BAT trigger was available only with the TAROT R-band and Konus-Wind (KW) data. Assuming a Gaussian function, Stratta et al. (2013) measured a peak epoch at (2460 ± 50) s after the BAT trigger with a width of ~ 130 s using the TAROT data, while a peak epoch at (2050 ± 10) s with a width consistent with the optical one using the KW data. Because there is no observations in X-ray band during the bump, we assume the peak time as $t_{\rm p} \sim 2500/(1+z)$ s based on the measurement of the peak epoch by Stratta et al. (2013) using the TAROT R-band and KW data.

In our calculation, we assume an efficiency of converting the BZ power to X-ray radiation as $\eta = 0.01$, and take the sharpness of the peak as $s = 1.9$. The BH is initially set up with a mass of $M_\bullet = 3M_\odot$ and a spin of $a_\bullet = 0.9$, just as assumed by Wu et al. (2013). Considering the luminosity at X-ray wavelength in the prompt phase, we assume the peak accretion rate as $\dot{M}_{\rm p} = 2.0 \times 10^{-4} M_\odot/{\rm s}$. To explain the plateau observed at X-ray wavelength in the early stage, we assumed a constant energy injection rate of $Q = 9.0 \times 10^{47}$ erg s^{-1} with the start and the end time of the energy injection as $t_{\rm start} = 8.0 \times 10^3$ s, $t_{\rm end} = 1.6 \times 10^4$ s respectively. The steep decay phase observed in X-ray band starting at about 20000 s is the end of the prompt phase and can be interpreted as the tail emission coming from high latitude (Kumar & Panaitescu 2000), whose decay index is $2 + \beta_{\rm X}$, where $\beta_{\rm X}$ is the spectral index in X-ray band. Figure 1 shows our fit to the X-ray bump in GRB 111209A and the calculation starts at $t_0 = 2000/(1+z)$ s.

4.2. Afterglows at late times

Paying special attention to the rebrightening of the afterglow of GRB 111209A in the optical band at around 10^5 s, we use the external shock with energy injection process to calculate the X-ray and optical afterglow light curves at late times in detail, and compare the numerical results with the observations. As the fluence of GRB 111209A measured in the 15 – 150 keV energy range by BAT is $(360 \pm 10) \times 10^{-7}$ erg cm^{-2}, the isotropic energy released in the rest-frame in the 15 – 150 keV band is then $E_{0,iso} = 4.3 \times 10^{52}$ erg. In our calculations, we will assume this value as the initial isotropic kinetic energy of the outflow. Other parameters are taken as following: the initial Lorentz factor of the blast wave $\gamma_0 = 60$, the ISM number density $n = 1.0$ cm^{-3}, the power-law index of the energy distribution of electrons $p = 2.25$, the electron energy fraction $\epsilon_e = 0.04$, the magnetic energy fraction $\epsilon_B = 0.004$, the initial half opening angle of the ejecta $\theta = 0.1$ radian, and the observing angle $\theta_{\rm obs} = 0$, where the observing angle is defined as the angle between the line of sight and the jet axis.

For the significant rebrightening at approximately 10^5 s after the trigger, possible theoretical interpretations were discussed in Stratta et al. (2013). In this paper, we assume another energy injection imposed on the external shock with $Q = 6.0 \times 10^{46}$ erg s^{-1}, $q = 0$, $t_{\rm start} = 6.5 \times 10^4$ s, and $t_{\rm end} = 8.1 \times 10^4$ s to interpret this significant rebrightening. This will lead to a total energy injection of $E_{\rm inj} = 2.3\ E_0$, where $E_0 = (1 - \cos\theta) E_{0,\rm iso}$ is the collimation-corrected energy. According to the analysis by Zhang & Mészáros (2002), such an injected energy higher than that of the original kinetic energy of the outflow should be able to generate an obvious rebrightening in the afterglow lightcurve.

Using the external shock mechanism and parameters described above, we can give a satisfactory fit to the observed X-ray and optical afterglow of GRB 111209A at late times. By superposing the theoretical luminosity in X-ray band from the fall back process in the early stage and that from the external shock at late times, we can get the complete fit to the whole observational data at X-ray wavelength. The observed X-ray and optical afterglow light curves of GRB 111209A and our best theoretical fit are illustrated in Figures 1 and 2 respectively. Using observational data from Stratta et al. (2013), we show that the multi-wavelength emission predicted by our model can well explain both the X-ray and optical data. It is interesting to note that in X-ray band, the theoretical amplitude of the rebrightening due to energy injection is much smaller as compared with that at optical wavelength. Although the X-ray rebrightening is not as significant as that in the optical band at about 10^5 s, our numerical result is reasonably consistent with the observed X-ray afterglow light curve.

Figure 2 illustrates the observed optical data of GRB 111209A at late times from Stratta et al. (2013). Also plotted are our calculated R band flux densities by using the same model as in Figure 1. We can see that the observed optical afterglow light curve can be satisfactorily reproduced.

It should be noted that in our calculations, we do not consider the reverse shock emission component during the energy injection stage. Actually, depending on different types of central

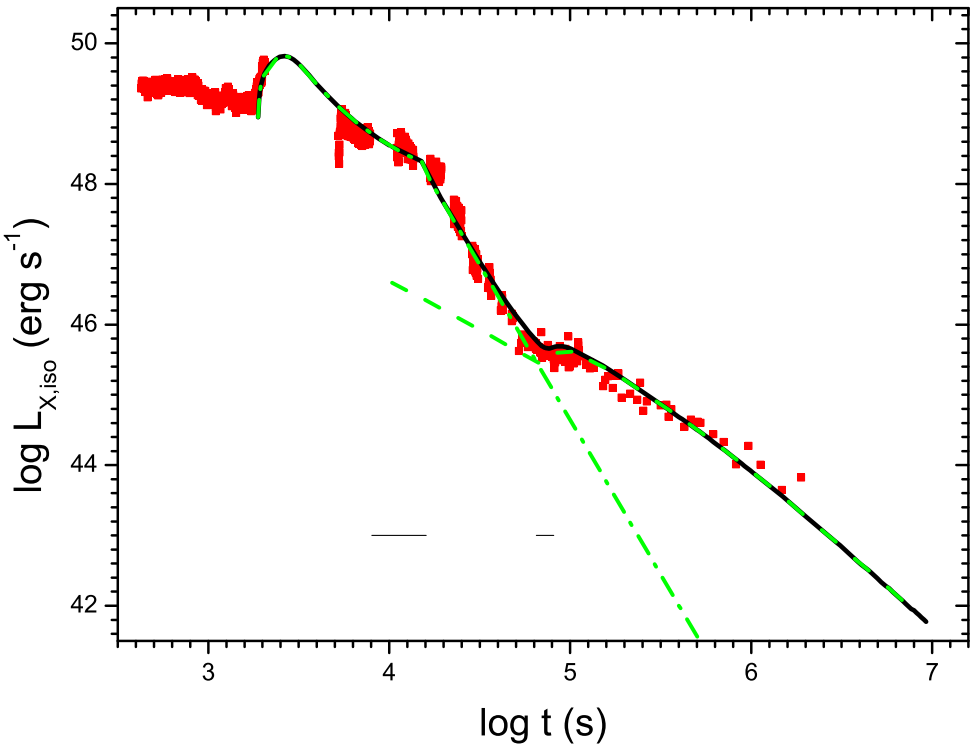

Fig. 1.— Numerical fit to the X-ray afterglow light curve of the ultra-long GRB 111209A, where the solid points represent the observed data from Stratta et al. (2013), and the dash dot line and dashed line correspond to the theoretical luminosity in X-ray band from fall back and external shock process respectively. The solid line is our overall theoretical light curve for GRB 111209A. The two straight lines at the bottom represent the start and stop epoches of the two energy injections phases.

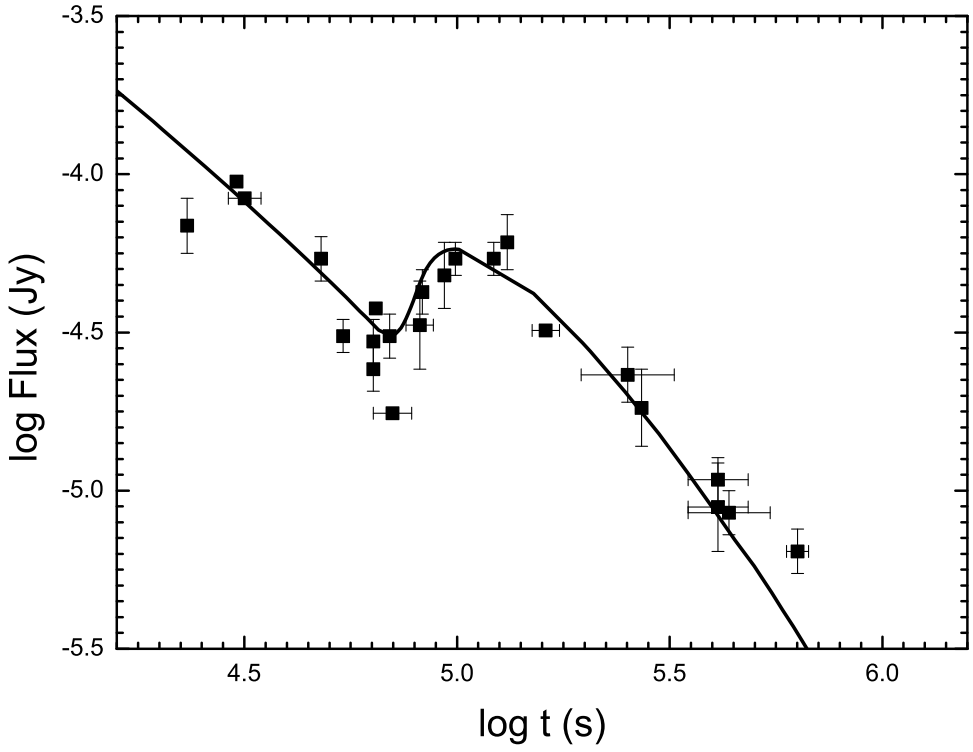

Fig. 2.— Numerical fit to the R-band optical afterglow of the ultra-long GRB 111209A at late times by using the same model as in Figure 1. The observational data are from Stratta et al. (2013). The solid line is our theoretical optical afterglow light curve corrected for extinction.

engines, the injected energy could be in a kinetic-energy-dominated form or in a Poynting-flux-dominated form (Usov 1994; Mészáros & Rees 1997b). When the injected energy is of a kinetic form, then during the injection process, reverse shocks might be produced. Emission from such reverse shocks could significantly enhance the rebrightenings (Zhang & Mészáros 2002). In realistic cases, it is also possible that when the fast shell catches up with the slow shell and gives birth to an energy injection, the relative speed between the two colliding shells is not too high, so that only a mildly relativistic reverse shock is generated (Rees & Mészáros 1998; Kumar & Piran 2000; Zhang & Mészáros 2002). In this case, emission from the reverse shock will not be very strong. In our modeling, the injection flows are assumed to be Poynting-flux-dominated, in which case, there will be no reverse shock generated during the injection process.

5. Discussion and Conclusions

GRBs are widely believed to be produced by relativistically expanding blastwaves at cosmological distances. The progenitors of long duration GRBs may be Wolf-Rayet stars (Chevalier & Li 1999) based on the Collapsar model (Woosley 1993). It is possible to observe early afterglows of many GRBs in the first few hours after the trigger due to the localization ability of the Swift satellite. Many remarkable and unexpected features such as rebrightenings in the optical afterglows have been observed, challenging the view that optical afterglow light curves should be smooth (Laursen & Stanek 2003), which was the accepted dogma before the discovery of the first GRB afterglow (e.g. Sahu et al. 1997).

GRB 111209A is characterized by complex afterglow light curves with an unprecedented burst duration of a few hours (Hoversten et al. 2011). Distinguishing features of this event include the significant bump at X-ray wavelength in the early stage and the obvious rebrightening in optical band at around 10^5 s after the burst. In this paper, we present a numerical study of the X-ray afterglow emission in the early stage, and compare our result with the observed X-ray afterglow light curve. It is shown that the observations can be fitted quite well by the fall back accretion model (Wu et al. 2013) with the appropriate choices of parameters. For the afterglows at late times, we calculate the overall dynamical evolution of the blastwave numerically by adding energy injection process to reproduce the X-ray and optical afterglow light curves of GRB 111209A. We assume that the relativistic shock expands in a uniform ISM. We show that the remarkable rebrightening observed in optical band can be satisfactorily reproduced by our model. We argue that the rapid rise is due to the energy injection generated by the central engine through BZ mechanism. In fact, energy injection mechanism has also been used to explain the afterglows of some other GRBs, such as GRB 010222 (Björnsson et al. 2002), GRB 021004 (Björnsson et al. 2004), GRB 021004 (de Ugarte Postigo et al. 2005), GRB 030329 (Huang et al. 2006; Deng et al. 2010), GRB 051221A (Fan & Xu 2006) and GRB 081029 (Yu & Huang 2013). In our calculations, many of the parameters, such as the power-law index of the energy distribution of electrons (p), the electron energy fraction (ϵ_e), the magnetic energy fraction (ϵ_B), the initial half opening angle of the ejecta (θ), have been

evaluated typically.

In our model, we have assumed two periods of energy injection, each with a constant injection power. One injection starts at 8.0×10^3 s and ends at 1.6×10^4 s, with an injection power of 9.0×10^{47} erg s^{-1}. This energy injection is mainly engaged to account for the plateau observed at X-ray wavelength in the early stage. The other injection starts at 6.5×10^4 s and ends at 8.1×10^4 s, with an injection power of 6.0×10^{46} erg s^{-1}. This energy injection can help to explain the plateau in X-ray band and the rebrightening in optical band at about 10^5 s. Physically, this kind of energy injection can be produced by the fallback of mass onto the central compact object of the burster as discussed by Yu & Huang (2013). The fall back is usually continuous, but clumps sometimes could form in the falling material. When a large clump suddenly plunges into the accretion disk, the accretion rate can be significantly increased, giving birth to a strong outflow. The relativistic shell resulted from the energetic outflow moves outward at approximately a constant speed in a dilute environment that has been swept-up by the previous external shock. It may eventually catch up with the fireball material and inject the energy into the external shock, producing a plateau or a rebrightening in the afterglow.

In our fitting to the optical afterglow of GRB 111209A, extinction has been taken into account. The theoretical light curve of GRB 111209A in the optical band was shifted downward by about 0.7 mag. It is consistent with the result derived by Stratta et al. (2013) who suggested that the rest frame visual dust extinction is $A_V = 0.3 - 1.5$ mag, which may be one possible reason for the non-detection of the accompanied supernova of GRB 111209A. Extinction has also been considered in many other GRBs. Sokolov et al (2001) pointed out that there is significant internal extinction in the host galaxies of GRBs 970508, 980613, 980703, 990123 and 991208. Rol et al (2007) suggested a high internal extinction, at least 2.3 magnitudes at the infrared (J) wavelength and 5.4 magnitudes at U band in the rest-frame to explain the absence of an optical afterglow for GRB 051022, which is a prototypical dark burst. Yu & Huang (2013) derived the extinction of the host galaxy of GRB 081029 as $A_V \sim 1.57$ mag by modeling the multi-band afterglow light curves. For high redshift GRBs, Draine (2000) draw the conclusion that absorption by vibrationally-excited H_2 could be responsible for the pronounced drop in flux between R and I band. Considering the fact that the redshift of GRB 111209A is about $z = 0.677$, absorption by H_2 may be another factor contributing to the extinction.

Another distinguishing feature of GRB 111209A is the long duration of the prompt emission, which is at least 25000 s as estimated by Gendre et al. (2013), using the start time of the detection by KW and the start time of the sharp decay. Based on the fact that the central engine can be kept active while the progenitor envelope is being accreted onto it (Kumar et al. 2008), the fall back accretion of a progenitor envelope (Quataert & Kasen 2012; Wu et al. 2013) may be one reasonable explanation for the long prompt emission duration of GRB 111209A. Woosley & Heger (2012) pointed out that direct envelope collapse of a massive star can produce GRBs with prompt emission lasting for about 10^4 s, therefore, a massive and extended progenitor like blue supergiant (Mészáros & Rees 2001) is another possible choice as the central engine of GRB 111209A. Gendre

et al. (2013) argued that the collapse of a blue supergiant is the best candidate for the progenitor of the ultra-long GRB 111209A, which was revised by Nakauchi et al. (2013) to explain the durations of ultra-long GRBs, such as GRBs 111209A, 101225A, and 121027A. Actually, considering the X-ray bump observed in the early stage and the ultra-long prompt emission duration, the mass fall back accretion is a more convincing model for GRB 111209A. Detailed theoretical models of the ultra-long GRB 111209A were discussed in Gendre et al. (2013).

In conclusion, we have shown that our model can reasonably explain both the X-ray and optical afterglow light curves of GRB 111209A. The observed X-ray bump in the early stage can be reproduced by the mass fall back process and the optical rebrightening at late times can be fitted quite well by assuming a constant energy injection. In the future, more detailed studies on the mass fall back and energy injection processes will provide important clues on the progenitors of GRBs, especially GRBs that show exceptional temporal features such as GRB 111209A.

This work was supported by the National Basic Research Program of China (973 Program, Grant No. 2009CB824800, 2014CB845800) and the National Natural Science Foundation of China (Grant No. 11033002). X.F. Wu acknowledges support by the One-Hundred Talents Program and the Youth Innovation Promotion Association of Chinese Academy of Sciences. D.M. Coward is supported by an Australian Research Council Future Fellowship. E.J. Howell acknowledges support from a UWA Research Fellowship.

REFERENCES

Bardeen, J. M., Press, W. H., & Teukolsky, S. A. 1972, ApJ, 178, 347

Bersier, D. 2012, arXiv:1206.6979

Bethe, H. A., Brown, G. E., & Lee, C.-H. 2007, Phys. Rep., 442, 5

Björnsson, G., Gudmundsson, E. H., & Jóhannesson, G. 2004, ApJ, 615, L77

Björnsson, G., Hjorth, J., Pedersen, K., & Fynbo, J. U. 2002, ApJ, 579, L59

Bloom, J. S., Sigurdsson, S., & Pols, O. R. 1999, MNRAS, 305, 763

Burrows, D. N., Romano, P., Falcone, A., et al. 2005, Science, 309, 1833

Chevalier, R. A. 1989, ApJ, 346, 847

Chevalier, R. A., & Li, Z.-Y. 2000, ApJ, 536, 195

Dai, Z. G., & Liu, R.-Y. 2012, ApJ, 759, 58

Dai, Z. G., & Lu, T. 1998, A&A, 333, L87

Dai, Z. G., & Lu, T. 2002, ApJ, 565, L87

Dai, Z. G., & Wu, X. F. 2003, ApJ, 591, L21

Dall'Osso, S., Stratta, G., Guetta, D., et al. 2011, A&A, 526, A121

de Ugarte Postigo, A., Castro-Tirado, A. J., Gorosabel, J., et al. 2005, A&A, 443, 841

Deng, W., Huang, Y.-F., & Kong, S.-W. 2010, Research in Astronomy and Astrophysics, 10, 1119

Draine, B. T. 2000, ApJ, 532, 273

Eichler, D., Livio, M., Piran, T., & Schramm, D. N. 1989, Nature, 340, 126

Fan, Y.-Z., & Xu, D. 2006, MNRAS, 372, L19

Fan, Y. Z., & Wei, D. M. 2005, MNRAS, 364, L42

Galama, T. J., Vreeswijk, P. M., van Paradijs, J., et al. 1998, Nature, 395, 670

Gehrels, N., Sarazin, C. L., O'Brien, P. T., et al. 2005, Nature, 437, 851

Gehrels, N., Ramirez-Ruiz, E., & Fox, D. B. 2009, ARA&A, 47, 567

Gendre, B., Stratta, G., Atteia, J. L., et al. 2013, ApJ, 766, 30

Geng, J. J., Wu, X.-F., Huang, Y.-F., & Yu, Y.-B. 2013, arXiv:1307.4517

Hoversten, E. A., Evans, P. A., Guidorzi, C., et al. 2011, GRB Coordinates Network, 12632, 1

Huang, Y. F., & Cheng, K. S. 2003, MNRAS, 341, 263

Huang, Y. F., Cheng, K. S., & Gao, T. T. 2006, ApJ, 637, 873

Huang, Y. F., Dai, Z. G., & Lu, T. 1998, A&A, 336, L69

Huang, Y. F., Dai, Z. G., & Lu, T. 1999a, Chinese Physics Letters, 16, 775

Huang, Y. F., Dai, Z. G., & Lu, T. 1999b, MNRAS, 309, 513

Huang, Y. F., Dai, Z. G., & Lu, T. 2000a, MNRAS, 316, 943

Huang, Y. F., Gou, L. J., Dai, Z. G., & Lu, T. 2000b, ApJ, 543, 90

Huang, Y. F., Lu, Y., Wong, A. Y. L., & Cheng, K. S. 2007, Chinese J. Astron. Astrophys., 7, 397

Huang, Y. F., Wu, X. F., Dai, Z. G., Ma, H. T., & Lu, T. 2004, ApJ, 605, 300

Janka, H. -., Ruffert, M., & Eberl, T. 1998, arXiv:astro-ph/9810057

Klebesadel, R. W., Strong, I. B., & Olson, R. A. 1973, ApJ, 182, L85

Kluźniak, W., & Ruderman, M. 1998, ApJ, 508, L113

Kong, S. W., & Huang, Y. F. 2010, Science China-Physics, Mechanics & Astronomy, 2010, 53(s1): 94-97

Kong, S. W., Wong, A. Y. L., Huang, Y. F., & Cheng, K. S. 2010, MNRAS, 402, 409

Kruehler, T., Tanvir, N. R., de Ugarte Postigo, A., et al. 2012, GRB Coordinates Network, 13930, 1

Kumar, P., Narayan, R., & Johnson, J. L. 2008, MNRAS, 388, 1729

Kumar, P., & Panaitescu, A. 2000, ApJ, 541, L9

Kumar, P., & Piran, T. 2000, ApJ, 532, 286

Laursen, L. T., & Stanek, K. Z. 2003, ApJ, 597, L107

Lazzati, D., Rossi, E., Covino, S., Ghisellini, G., & Malesani, D. 2002, A&A, 396, L5

Lee, H. K., Wijers, R. A. M. J., & Brown, G. E. 2000, Phys. Rep., 325, 83

Lei, W.-H., & Zhang, B. 2011, ApJ, 740, L27

Liu, X. W., Wu, X. F., & Lu, T. 2008, A&A, 487, 503

MacFadyen, A. I., & Woosley, S. E. 1999, ApJ, 524, 262

MacFadyen, A. I., Woosley, S. E., & Heger, A. 2001, ApJ, 550, 410

McKinney, J. C. 2005, ApJ, 630, L5

Mészáros, P. 2002, ARA&A, 40, 137

Mészáros, P., & Rees, M. J. 1997a, ApJ, 476, 232

Mészáros, P., & Rees, M. J. 1997b, ApJ, 482, L29

Mészáros, P., & Rees, M. J. 2001, ApJ, 556, L37

Nakar, E. 2007, Phys. Rep., 442, 166

Nakauchi, D., Kashiyama, K., Suwa, Y., & Nakamura, T. 2013, arXiv:1307.5061

Narayan, R., Paczynski, B., & Piran, T. 1992, ApJ, 395, L83

Nava, L., Sironi, L., Ghisellini, G., Celotti, A., & Ghirlanda, G. 2013, MNRAS, 433, 2107

Novikov, I. D., & Thorne, K. S. 1973, Black Holes (Les Astres Occlus), 343

Paczynski, B. 1998, ApJ, 494, L45

Pe'er, A. 2012, ApJ, 752, L8

Perna, R., & Belczynski, K. 2002, ApJ, 570, 252

Piran, T. 1999, Phys. Rep., 314, 575

Piran, T. 2000, Phys. Rep., 333, 529

Quataert, E., & Kasen, D. 2012, MNRAS, 419, L1

Rees, M. J., & Mészáros, P. 1994, ApJ, 430, L93

Rees, M. J., & Mészáros, P. 1998, ApJ, 496, L1

Rhoads, J. E. 1999, ApJ, 525, 737

Rol, E., van der Horst, A., Wiersema, K., et al. 2007, ApJ, 669, 1098

Rowlinson, A., O'Brien, P. T., Metzger, B. D., Tanvir, N. R., & Levan, A. J. 2013, MNRAS, 430, 1061

Sahu, K. C., Livio, M., Petro, L., et al. 1997, Nature, 387, 476

Sari, R., & Esin, A. A. 2001, ApJ, 548, 787

Sari, R., Piran, T., & Halpern, J. P. 1999, ApJ, 519, L17

Sari, R., Piran, T., & Narayan, R. 1998, ApJ, 497, L17

Sokolov, V. V., Fatkhullin, T. A., Castro-Tirado, A. J., et al. 2001, A&A, 372, 438

Sokolov, V. V., Zharikov, S. V., Baryshev, Y. V., et al. 1999, A&A, 344, 43

Stratta, G., Gendre, B., Atteia, J. L., et al. 2013, arXiv:1306.1699

Tam, P. H., Pun, C. S. J., Huang, Y. F., & Cheng, K. S. 2005, New Astronomy, 10, 535

Tutukov, A. V., & Fedorova, A. V. 2007, Astronomy Reports, 51, 291

Usov, V. V. 1994, MNRAS, 267, 1035

van Eerten, H. J., Leventis, K., Meliani, Z., Wijers, R. A. M. J., & Keppens, R. 2010, MNRAS, 403, 300

Vreeswijk, P., Fynbo, J., & Melandri, A. 2011, GRB Coordinates Network, 12648, 1

Wang, D. X., Xiao, K., & Lei, W. H. 2002, MNRAS, 335, 655

Wei, D. M., & Lu, T. 2000, A&A, 360, L13

Woosley, S. E. 1993, ApJ, 405, 273

Woosley, S. E., & Heger, A. 2012, ApJ, 752, 32

Woźniak, P. R., Vestrand, W. T., Wren, J. A., et al. 2006, ApJ, 642, L99

Wu, X.-F., Hou, S.-J., & Lei, W.-H. 2013, ApJ, 767, L36

Yu, Y.-B., & Huang, Y.-F. 2013, Research in Astronomy and Astrophysics, 13, 662

Zhang, B. 2007, Chinese J. Astron. Astrophys., 7, 1

Zhang, B., Fan, Y. Z., Dyks, J., et al. 2006, ApJ, 642, 354

Zhang, B., & Mészáros, P. 2001a, ApJ, 552, L35

Zhang, B., & Mészáros, P. 2001b, ApJ, 559, 110

Zhang, B., & Mészáros, P. 2002, ApJ, 566, 712

Zhang, W., Woosley, S. E., & Heger, A. 2008, ApJ, 679, 639